

# On the Nature and Incidence of $\beta$ -Agostic Interactions in Ethyl Derivatives of Early Transition Metals: Ethyltitanium Trichloride and Related Compounds

Arne Haaland,<sup>†</sup> Wolfgang Scherer,<sup>\*,‡</sup> Kenneth Ruud,<sup>†</sup> G. Sean McGrady,<sup>\*,⊥</sup> Anthony J. Downs,<sup>⊥</sup> and Ole Swang<sup>§</sup>

Contribution from the Department of Chemistry, University of Oslo, Box 1033 Blindern, N-0315 Oslo, Norway, Anorganisch-chemisches Institut, Technische Universität München, Lichtenbergstrasse 4, D-85747 Garching, Germany, Inorganic Chemistry Laboratory, University of Oxford, South Parks Road, Oxford OX1 3QR, UK, and SINTEF, Applied Chemistry, Department of Hydrocarbon Process Chemistry, Box 124 Blindern, N-0314 Oslo, Norway

Received October 30, 1997

**Abstract:** In light of the structures and spectroscopic properties of the ethyltitanium compounds EtTiCl<sub>3</sub> (**1**), and EtTiCl<sub>3</sub>(dmpe) (dmpe = Me<sub>2</sub>PCH<sub>2</sub>CH<sub>2</sub>PMe<sub>2</sub>) (**2**), extensive DFT calculations have been carried out to explore the structures, energetics, potential energy surfaces, and spectroscopic properties not only of these but also of related ethyl derivatives of early transition metals, M. The analysis has sought to assess the true nature of so-called  $\beta$ -agostic interactions in these systems and how such interactions depend on the atomic number, coordination number, valence electron (VE) count, and net charge of M. The calculations reproduce well the experimentally determined properties of **1** and **2**. Analysis of wave functions indicates that, where significant  $\beta$ -interactions occur, the M–C <sub>$\alpha$</sub>  bonding electrons are delocalized over the entire ethyl group, the marked reduction of the MCC valence angle allowing the metal atom to establish covalent bonding interactions with the  $\beta$ -C atom and, perhaps to a lesser extent, with its appended proximal H atom. A  $\beta$ -agostic alkyl group may be considered a two-electron ligand, and the main contribution to the stabilization arises from Ti $\cdots$ C <sub>$\beta$</sub>  bonding. Barriers to conformational change of the M–Et unit depend inter alia on the space available in the coordination sphere of the central M atom, with rearrangement of the ethyl group to accommodate significant  $\beta$ -interaction being opposed by interligand repulsion. Such interaction is found not in **1**, but in its dmpe adduct **2** because the increase in coordination number is offset by elongation of the Ti–C and Ti–Cl bonds and by the extra pliability of the EtTiCl<sub>3</sub> moiety resulting from complexation by the dmpe ligand.

## 1. Introduction

The apparent attraction between a transition metal center and a CH fragment in an organic ligand is commonly referred to as an “agostic” interaction. More specifically, the attraction between a transition metal M and the  $\beta$ -CH fragment of an appended alkyl ligand is termed  $\beta$ -agostic.<sup>1</sup>  $\beta$ -Interactions appear to be the most prevalent type reported,<sup>1</sup> presumably on account of the favorable geometry enjoyed by such an arrangement. The primary structural evidence of a  $\beta$ -agostic interaction is a reduction of the MC <sub>$\alpha$</sub> C <sub>$\beta$</sub>  valence angle, in several cases to values below 90°. Agostic interactions may also be signaled by a significant reduction in the C–H stretching frequency, although only in a few cases has the identity of the mode been authenticated.<sup>1,2a</sup> In addition, a low-frequency shift of the <sup>1</sup>H resonance and a reduced C,H coupling constant in the NMR spectrum are taken to be diagnostic of agostic behavior.<sup>1,2a</sup> The

evidence for agostic interactions accumulated up to 1988 has been the subject of two seminal reviews.<sup>1</sup>

Increased knowledge about these interactions is vital to a proper understanding of several important chemical reactions involving transition-metal compounds and organic molecules, where products, intermediates, and transition states may be stabilized in this manner. Thus, olefin insertion into M–H bonds and the reverse reaction—olefin elimination from transition-metal alkyls—are both believed to proceed through  $\beta$ -agostic transition states.<sup>2b</sup> Similarly, the industrial production of aldehydes from olefins, CO, and H<sub>2</sub> with HCo(CO)<sub>4</sub> as a catalyst is believed to proceed through the formation of two  $\beta$ -agostic intermediates.<sup>3</sup> Such interactions may also be present in the resting state of the cationic species derived from Group 4 metallocenes which are catalytically active in the promotion of olefin polymerization.<sup>4</sup>

Agostic interactions have in the past been envisaged as involving the donation of a C–H bonding electron pair to the metal atom M.<sup>1</sup> On this basis, the alkyl ligand is to be regarded as a four-electron ligand. It is an essential prerequisite,

<sup>†</sup> University of Oslo.

<sup>‡</sup> Technische Universität München.

<sup>⊥</sup> University of Oxford.

<sup>§</sup> SINTEF.

(1) (a) Brookhart, M.; Green, M. L. H. *J. Organomet. Chem.* **1983**, *250*, 395–408. (b) Brookhart, M.; Green, M. L. H.; Wong, L.-L. *Prog. Inorg. Chem.* **1988**, *36*, 1–124.

(2) (a) Elschenbroich, Ch.; Salzer, A. *Organometallics*, 2nd ed.; VCH: Weinheim, Germany, 1992; pp 267–268. (b) Elschenbroich, Ch.; Salzer, A. *Organometallics*, 2nd ed.; VCH: Weinheim, Germany, pp 186–191. (c) Elschenbroich, Ch.; Salzer, A. *Organometallics*, 2nd ed.; VCH: Weinheim, Germany, pp 198–200.

(3) Ziegler, T. *Can. J. Chem.* **1995**, *73*, 743–761.

(4) (a) Brintzinger, H. H.; Fischer, D.; Mülhaupt, R.; Rieger, B.; Waymouth, R. M. *Angew. Chem., Int. Ed. Engl.* **1995**, *34*, 1143–1170. (b) Woo, T. K.; Fan, L.; Ziegler, T. *Organometallics* **1994**, *13*, 2252–2261. (c) Woo, T. K.; Margl, P. M.; Lohrenz, J. C. W.; Blöchl, P. E.; Ziegler, T. *J. Am. Chem. Soc.* **1996**, *118*, 13021–13030.

moreover, that M carry a vacant valence orbital having an energy and disposition that are compatible with those of the C–H bonding orbital;  $M\cdots H-C$  attractions should therefore be favored if the formal valence electron (VE) count for M is 16 or less. The dative character of the interaction also suggests that agostic behavior will be favored if M carries a net positive charge.

Two compounds provide experimental benchmarks for consideration of  $\beta$ -agostic interactions. These are ethyltitanium trichloride,  $EtTiCl_3$  (**1**), with a VE count of 8, and its complex  $EtTiCl_3(dmpe)$  ( $dmpe = Me_2PCH_2CH_2PMe_2$ ) (**2**) with a VE count of 12. Electron diffraction measurements on gaseous **1** indicate an anagostic structure with  $\angle TiCC = 116.6(11)^\circ$  and a staggered ethyl group geometry (here and henceforth the ethyl group conformation is defined with respect to the  $Ti-C_\alpha$  bond).<sup>5</sup> Neither these dimensions nor the vibrational<sup>6</sup> and NMR properties give the slightest hint of agostic behavior. Yet the crystal structure of the diphosphine complex **2**, as redetermined at low temperature (105 K),<sup>5</sup> clearly manifests such behavior; in addition, the vibrational<sup>6</sup> and NMR properties exhibit unusual features that can be interpreted only on the assumption that complexation induces a significant change not just in the  $TiC_\alpha C_\beta$  valence angle but in the bonding of the whole ethyl ligand. Central to our analysis of the results reported to date have been Density Functional Theory (DFT) calculations; these have sought to enquire into the equilibrium structures, MCC bending potentials, ethyl group conformations, and  $M-C_2H_5$  bonding modes in **1**, **2**, and several related species. Here we report in detail on the results of the analysis, with particular reference to the light they shed on the true nature of  $\beta$ -agostic bonding and on the factors giving rise to such bonding.

## 2. Results and Discussion

**2.1. Structures of Ethyl-transition Metal Compounds: A Survey.** A survey based on the Cambridge Crystal Structure File (Release 5.10)<sup>7a,b</sup> but augmented by a literature search<sup>7c,d</sup> has yielded the structures of 58 complexes of transition metals M drawn from Groups 3–11 and bearing terminal ethyl groups. Out of these 29 involve M atoms with a formal count of 16 or fewer VE, 24 being neutral compounds and five cationic species. From all the 24 neutral complexes *only one*, viz. the 12 VE compound  $EtTiCl_3(dmpe)$  (**2**), displays clear signs of a  $\beta$ -agostic interaction. According to the latest study,<sup>5</sup> the  $TiC_\alpha C_\beta$  angle at  $84.57(9)^\circ$  is conspicuously acute; the orientation of the ethyl group is such that one  $C_\beta-H$  bond eclipses the  $Ti-C_\alpha$  bond giving a  $Ti\cdots H$  distance of only  $206(2)$  pm.<sup>5</sup> Out of the five cationic ethyl complexes no less than four exhibit acute  $MC_\alpha C_\beta$  angles suggestive of  $\beta$ -agostic interactions, viz.  $[EtPt\{Bu'_2P(CH_2)_3PBu'_2\}]^+$ ,<sup>7c</sup> VE = 14,  $\angle PtC_\alpha C_\beta = 75(1)^\circ$ ;  $[EtNi\{Bu'_2P(CH_2)_2PBu'_2\}]^+$ ,<sup>8a</sup> VE = 14,  $\angle NiC_\alpha C_\beta = 74.5(3)^\circ$ ;  $[EtCo(\eta-Cp^*)\{P(p-tolyl)_3\}]^+$  ( $Cp^* =$  pentamethylcyclopentadienyl),<sup>8b</sup> VE = 16,  $\angle CoC_\alpha C_\beta = 74.5(2)^\circ$ ; and  $[EtZr(\eta-C_5H_4Me)_2(PMe_3)]^+$ ,<sup>8c</sup> VE = 16, two independent molecules in the asymmetric unit cell with  $\angle ZrC_\alpha C_\beta = 84.7(5)$  and  $83.0(6)^\circ$ , respectively.

(5) Scherer, W.; Priemeier, T.; Haaland, A.; Volden, H.-V.; McGrady, G. S.; Downs, A. J.; Boese, R.; Bläser, D. *Organometallics* Submitted for publication.

(6) McGrady, G. S.; Downs, A. J.; Haaland, A.; Scherer, W.; McKean, D. C. *J. Chem. Soc., Chem. Commun.* **1997**, 1547–1548.

(7) (a) Allen, F. H.; Kennard, O.; Taylor, R. *Acc. Chem. Res.* **1983**, *16*, 146–153. (b) A study of  $M\cdots H-C$  interaction geometries in some 50 transition metal compounds from the Cambridge Structural Database has recently been published: Braga, D.; Grepioni, F.; Biradha, K.; Desiraju, G. R. *J. Chem. Soc., Dalton Trans.* **1996**, 3925–3930. (c) Mole, L.; Spencer, J. L.; Carr, N.; Orpen, A. G. *Organometallics* **1991**, *10*, 49–54. (d) Davies, C. E.; Gardiner, I. M.; Green, J. C.; Green, M. L. H.; Hazel, N. J. *J. Chem. Soc., Dalton Trans.* **1985**, 669–683.

With regard to coordination number, the metal atoms in  $[EtPt\{Bu'_2P(CH_2)_3PBu'_2\}]^+$  and  $[EtNi\{Bu'_2P(CH_2)_3PBu'_2\}]^+$  are three-coordinate, and, if we regard the  $Cp^*$  ligand as occupying one coordination site, so too is the metal atom in  $[EtCo(\eta-Cp^*)\{P(p-tolyl)_3\}]^+$ . These are, in fact, the only three-coordinate metal complexes in our sample; all are cationic and all are evidently agostic. Although the crystal structures have not been determined, two *neutral pseudo-tri-coordinated* complexes are reported to show  $\beta$ -agostic behavior: IR spectroscopy<sup>9a</sup> and kinetic studies<sup>9b</sup> on the 14 VE metallocene  $Cp^*_2ScEt$  and IR, EPR, and electronic spectroscopy<sup>10a,b</sup> on the 15 VE metallocene  $Cp^*_2TiEt$  point to the presence of weak agostic interactions in both compounds. The cationic zirconium complex  $[EtZr(\eta-C_5H_4Me)_2(PMe_3)]^+$  is one of only two cationic complexes and the only one out of a total of 19 four-coordinate complexes in our sample to manifest agostic behavior. None of the five five-coordinate complexes (all neutral) appears to be agostic. That leaves three six-coordinate complexes (all neutral) of which only one, viz. the 12 VE  $EtTiCl_3(dmpe)$  (**2**) is agostic.<sup>5,6,14</sup> These findings suggest that, while  $\beta$ -agostic interactions may be common in three-coordinate complexes, they are rare in four-coordinate and perhaps also in five- or six-coordinate compounds. Furthermore, these same interactions may be better favored in cationic than in neutral species.

When we turn our attention to the 29 ethyl-transition metal complexes with  $VE > 16$ , we find that none is three-coordinate; four are either four- or five-coordinate, all of them neutral; the remaining 25 are six-coordinate, six of them being cationic. However, not one of the 29 complexes shows signs of agostic properties. It is evident therefore that the complex  $EtTiCl_3(dmpe)$  is *unique* in being a six-coordinate complex featuring a  $\beta$ -agostic structure and insofar as it is possible to generalize on the basis of a sample containing only one such structure, the data available suggest that  $\beta$ -agostic interactions are better favored in complexes with  $VE \leq 16$ . We note, however, that only 12 of these complexes are early transition-metal systems, two of which are agostic and that the *exceptionally* low VE count for  $EtTiCl_3(dmpe)$  may be significant.

**2.2. The Properties of  $EtTiCl_3$  (**1**).** Ethyltitanium trichloride,  $EtTiCl_3$  (**1**), is formally an 8 VE compound. In view of the behavior of the more electron-rich complex  $EtTiCl_3(dmpe)$  (**2**) the base-free molecule might be expected to display, if anything, an even more robust  $\beta$ -interaction.<sup>1</sup> The reality, as

(8) (a) Conroy-Lewis, F. M.; Mole, L.; Redhouse, A. D.; Litster, S. A.; Spencer, J. L. *J. Chem. Soc., Chem. Commun.* **1991**, 1601–1603. While the NMR spectra of  $[EtNi\{Bu'_2P(CH_2)_3PBu'_2\}]^+$  indicate that it retains the  $\beta$ -agostic alkyl group in solution, those of the Pt analogue, whose crystal structure is unknown, suggest a rapidly equilibrating mixture of  $\beta$ -agostic alkyl and an ethylene hydride complex,  $[C_2H_4(H)Pt\{Bu'_2P(CH_2)_3PBu'_2\}]^+$ . (b) Cracknell, R. B.; Orpen, A. G.; Spencer, J. L. *J. Chem. Soc., Chem. Commun.* **1984**, 326–328. (c) Jordan, R. F.; Bradley, P. K.; Baenziger, N. C.; LaPointe, R. E. *J. Am. Chem. Soc.* **1990**, *112*, 1289–1291.

(9) (a) Thompson, M. E.; Baxter, S. M.; Bulls, A. R.; Burger, B. J.; Nolan, M. C.; Santarsiero, B. D.; Schaefer, W. P.; Bercaw, J. E. *J. Am. Chem. Soc.* **1987**, *109*, 203–219. (b) Burger, B. J.; Thompson, M. E.; Cotter, W. D.; Bercaw, J. E. *J. Am. Chem. Soc.* **1990**, *112*, 1566–1577.

(10) (a) Luinstra, G. A.; ten Cate, L. C.; Heeres, H. J.; Pattiasina, J. W.; Meetsma, A.; Teuben, J. H. *Organometallics* **1991**, *10*, 3227–3237. (b) Lukens, W. W., Jr.; Smith, M. R., III; Andersen, R. A. *J. Am. Chem. Soc.* **1996**, *118*, 1719–1728.

(11) Scherer, W.; Haaland, A.; Herrmann, W. A.; Geisberger, M. Unpublished results.

(12) (a) McKean, D. C.; McQuillan, G. P.; Robertson, A. H. J.; Murphy, W. F.; Mastryukov, V. S.; Boggs, J. E. *J. Phys. Chem.* **1995**, *99*, 8994–9002. (b) Suzuki, S.; Bribes, J. L.; Gaufrès, R. *J. Mol. Spectrosc.* **1973**, *47*, 118–125.

(13) Bondi, A. J. *J. Phys. Chem.* **1964**, *68*, 441–451.

(14) Dawoodi, Z.; Green, M. L. H.; Mtetwa, V. S. B.; Prout, K.; Schultz, A. J.; Williams, J. M.; Koetzle, T. F. *J. Chem. Soc., Dalton Trans.* **1986**, 1629–1637.

**Table 1.** Relevant Structural Parameters of EtTiCl<sub>3</sub>(dmpe) (**2**) and EtTiCl<sub>3</sub>(dhpe) (**2a**)

parameter <sup>a</sup>	<b>2</b>	<b>2</b>	<b>2</b>	<b>2</b>	<b>2a</b>
	X-ray 105 K	BP86/III eclipsed	BP86/III staggered	BP86/III staggered	BPW91/I eclipsed
$\Delta E_{\text{rel}}^b$		0	0.177	1.84 <sup>c</sup>	
$\angle\text{TiCC}$	84.57(9)	85.5	93.10	112.0	85.4
Ti–C	214.7(1)	217.0	216.0	215.1	216.1
Ti···C <sub>β</sub>	250.1(2)	254.9	271.5	307.4	253.9
C <sub>α</sub> –C <sub>β</sub>	150.1(2)	151.7	153.4	153.4	151.9
C–H <sub>β</sub> <sup>f</sup>	103(2)	113.0	110.7	110.5	113.0
C–H <sub>β</sub> <sup>g,d</sup>	98(2)	110.0	110.2	110.1	109.8
Ti–Cl(1)	241.54(4)	238.9	232.6	228.4	236.4
Ti–Cl(2)	231.54(4)	233.0	233.9	233.8	233.6
Ti–P(1)	255.56(4)	258.5	260.6	263.8	256.7
Ti–P(2)	257.27(4)	258.6	258.8	263.8	259.6
$\angle\text{CCH}_\beta^f$	112.3(10)	114.2	110.6	110.3	114.6
$\angle\text{CTiCl}(1)$	129.61(4)	129.3	123.3	115.3	130.5
$\angle\text{CTiP}(1)$	74.84(4)	75.9	76.4	78.7	74.5
$\angle\text{CTiP}(2)$	149.53(4)	151.6	151.8	153.2	148.9
$\angle\text{CTiCl}(2)$	89.92(5)	89.7	90.5	90.4	90.6
$\angle\text{Cl}(2)\text{TiCl}(3)$	172.31(2)	167.4	165.4	162.7	164.7
$\angle\text{P}(1)\text{TiP}(2)$	74.98(1)	75.9	75.6	74.9	74.5
$\angle\text{P}(2)\text{TiCl}(1)$	80.77(1)	79.1	84.8	91.3	80.6
$\tau_{\text{C}_\beta\text{C}_\alpha\text{TiCl}(1)}$	–3.88(9)	–7.8	–4.5	–20.2	–5.1
$\tau_{\text{H}_\beta\text{C}_\beta\text{C}_\alpha\text{Ti}}$	1.4(12)	0.1	179.8	175.8	–1.5

<sup>a</sup> Atom in the symmetry plane is denoted by ('); atom out of the symmetry plane is denoted by ("). <sup>b</sup>  $E$  in kcal mol<sup>–1</sup>. <sup>c</sup> Constrained value. <sup>d</sup> Averaged value.

revealed by electron diffraction<sup>5</sup> and vibrational<sup>6</sup> and NMR spectroscopies, confounds this expectation. For the gaseous molecule **1** has a normal structure with  $C_s$  symmetry overall; the ethyl group assumes a staggered conformation about the C–C bond, with the bond distances ( $r_a$  in pm) Ti–C = 209.0(15), C–C = 152.6(11), and Ti–Cl = 219.5(3) and the valence angles (in deg)  $\angle\text{TiCC} = 116.6(11)$  and  $\angle\text{CITiC} = 104.6(4)$ . The structural parameters thus signify the absence of a significant  $\beta$ -agostic interaction. Indeed, the magnitude of the TiCC angle suggests that the C<sub>β</sub>H<sub>3</sub> group is not so much attracted to the metal center as repelled by the Cl atoms in gauche positions. Neither the IR<sup>6</sup> nor the <sup>1</sup>H and <sup>13</sup>C NMR spectra suggest anything other than a normal or agostic structure.

DFT structure optimizations carried out without imposition of molecular symmetry also converged to a model with  $C_s$  symmetry and with the TiC<sub>2</sub>H<sub>5</sub> group in a staggered conformation about the C–C bond. The energy obtained by optimization of a  $C_s$  model in which the TiC<sub>2</sub>H<sub>5</sub> group was locked in an eclipsed conformation was 1.7 kcal mol<sup>–1</sup>, so that the calculations on this and other ethyl–metal compounds (e.g., EtReO<sub>3</sub><sup>11</sup>) favor equilibrium structures that are staggered. The parameters calculated for **1**, listed in Table 5, are in close agreement with those determined experimentally.<sup>5</sup> In fact, the optimized eclipsed model corresponds not to a minimum on the potential energy surface but to a saddle-point. The rotation of the methyl group into an eclipsed conformation brings one methyl group hydrogen atom closer to the metal atom. At the same time, the optimal TiCC angle is reduced by 5° to 112.2°.

Perhaps the most striking result to emerge from the experimental and computational studies of EtTiCl<sub>3</sub> is the extreme pliability of the TiC<sub>2</sub>H<sub>5</sub> moiety. In Table 2 we compare the E–C and C–C stretching force constants and ECC bending force constants for the compounds EtCl,<sup>12a</sup> EtBr,<sup>12b</sup> EtReO<sub>3</sub>,<sup>11</sup> and EtTiCl<sub>3</sub>, where E = Cl, Br, Re, or Ti. Both the E–C stretching and ECC bending force constants are seen to decrease markedly in the sequence E = Cl > Br > Re > Ti corresponding to increasing polarization of the E–C<sub>2</sub>H<sub>5</sub> fragment. The

**Table 2.** Comparison of Principal Force Constants in Selected Ethyl Compounds

molecule	force constant <sup>a</sup> (N m <sup>–1</sup> )		
	E–C <sup>b</sup>	C–C stretching	ECC bending <sup>b</sup>
EtCl <sup>c</sup>	323.9	445.3	95.7
EtBr <sup>d</sup>	244.9	456.1	98.9
EtReO <sub>3</sub> <sup>e</sup>	235.2	401.9	49.8
EtTiCl <sub>3</sub> <sup>f</sup>	180.9	404.1	28.2

<sup>a</sup> Force constants were obtained from the scaled Cartesian force field. See Experimental Section for further information. <sup>b</sup> E = Cl, Br, Re, or Ti. <sup>c</sup> Reference 12a. <sup>d</sup> Reference 12b. <sup>e</sup> Reference 11. <sup>f</sup> This work.

adiabatic TiCC bending potential in EtTiCl<sub>3</sub> was further explored by fixing the TiCC angle at values ranging from 120 to 87° and carrying out DFT optimization of all the other structure parameters under retention of  $C_s$  symmetry. The resulting potential energy curve is shown in Figure 1. Hence it appears that an energy input of no more than 2.8 kcal mol<sup>–1</sup> (i.e., an amount equal to the rotational barrier in ethane) is needed to reduce the TiCC angle by 20°. The potential energy curve for the eclipsed conformer is even softer: reduction of the TiCC angle by 20° now requires an energy input of less than 1.5 kcal mol<sup>–1</sup>. As a result, the eclipsed conformer is favored over the staggered one for TiCC angles less than 97° (see Figure 1).

The nonbonded C<sub>β</sub>···Cl'' distance in the calculated equilibrium structure is 383 pm, slightly larger than the sum of the van der Waals' radii of a methyl group and a Cl atom, namely 375 pm.<sup>13</sup> Optimization of a model with an eclipsed ethyl group conformation and the TiCC valence angle fixed at 87° leads to a calculated distance of 343 pm. At the same time, the coordination geometry of the Ti atom distorts in a manner indicative of C<sub>β</sub>H<sub>3</sub>···Cl'' repulsion; the two C<sub>α</sub>TiCl'' valence angles increase while the C<sub>α</sub>TiCl' valence angle decreases. We suggest therefore that the extreme pliability of the Ti–C–C skeleton in **1** is due to the near-cancellation of two opposing forces, i.e.,  $\beta$ -agostic attraction, which favors a small angle, and C<sub>β</sub>H<sub>3</sub>···Cl'' repulsion, which favors a large one.

We now turn to a discussion of the bonding and begin by describing the frontier molecular orbitals derived from calculations on the [C<sub>2</sub>H<sub>5</sub>]<sup>–</sup> anion and [TiCl<sub>3</sub>]<sup>+</sup> cation (see Figure 2). A constant density contour map of the LUMO of the [TiCl<sub>3</sub>]<sup>+</sup> ion is shown on the left; it corresponds to a nearly pure d<sub>z</sub><sup>2</sup> metal atom orbital. A similar diagram of the HOMO of the [C<sub>2</sub>H<sub>5</sub>]<sup>–</sup> anion is shown on the right; as a first rough approximation, it may be regarded as an sp<sup>3</sup> lone pair orbital on C<sub>α</sub> but considerably delocalized. This orbital may be considered to be derived from one of the degenerate HOMO's of ethane by removal of H<sup>+</sup> from the  $\alpha$ -C atom or to be derived from ethylene by addition of H<sup>–</sup> to the  $\beta$ -C atom. Accordingly, it is very similar to one of the HOMO's of C<sub>2</sub>H<sub>6</sub> and to the corresponding LUMO of C<sub>2</sub>H<sub>4</sub>. The orbital is C–C antibonding but C–H bonding, and in the following account we shall refer to it as the  $\pi_z^*$  orbital of the ethyl ligand. Contour maps of the HOMO and LUMO of EtTiCl<sub>3</sub> are shown in the center of Figure 2. Both these orbitals have A' symmetry. The HOMO is a Ti–C  $\sigma$ -bond orbital formed by combination of the Ti d<sub>z</sub><sup>2</sup> orbital and the  $\pi_z^*$  orbital of the ethyl group: the main bonding interaction is clearly between Ti and C<sub>α</sub>, with a slight antibonding interaction between the metal atom and the C<sub>β</sub> and H<sub>β</sub> atoms. This antibonding character is, of course, in keeping with the wide TiCC valence angle.

**2.3. The Properties of EtTiCl<sub>3</sub>(dmpe) (**2**) and the Model Compound EtTiCl<sub>3</sub>(dhpe) (**2a**).** The molecular structure determined for a single crystal of a carefully prepared sample of the adduct EtTiCl<sub>3</sub>(dmpe) (**2**) at 105 K<sup>5</sup> indicates the

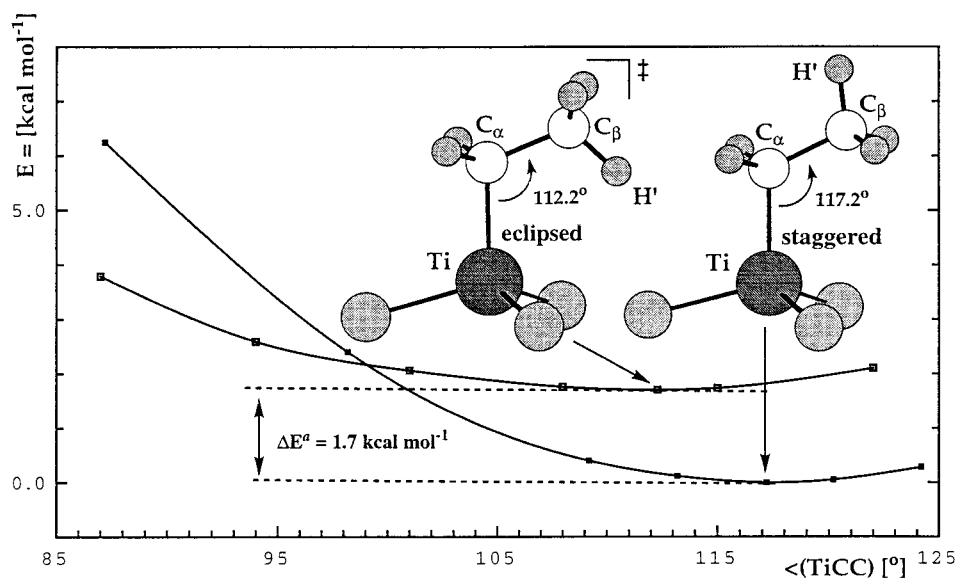


**Figure 1.** Variation of the total energy with the TiCC angle in EtTiCl<sub>3</sub> (**1**) for eclipsed and staggered conformers. Superscript footnote *a*: correction for zero point vibrational energy yields  $\Delta E_v = 1.5 \text{ kcal mol}^{-1}$ . The primes indicate the location of an atom either in (') or out of (") the  $C_s$  symmetry plane of the molecule.

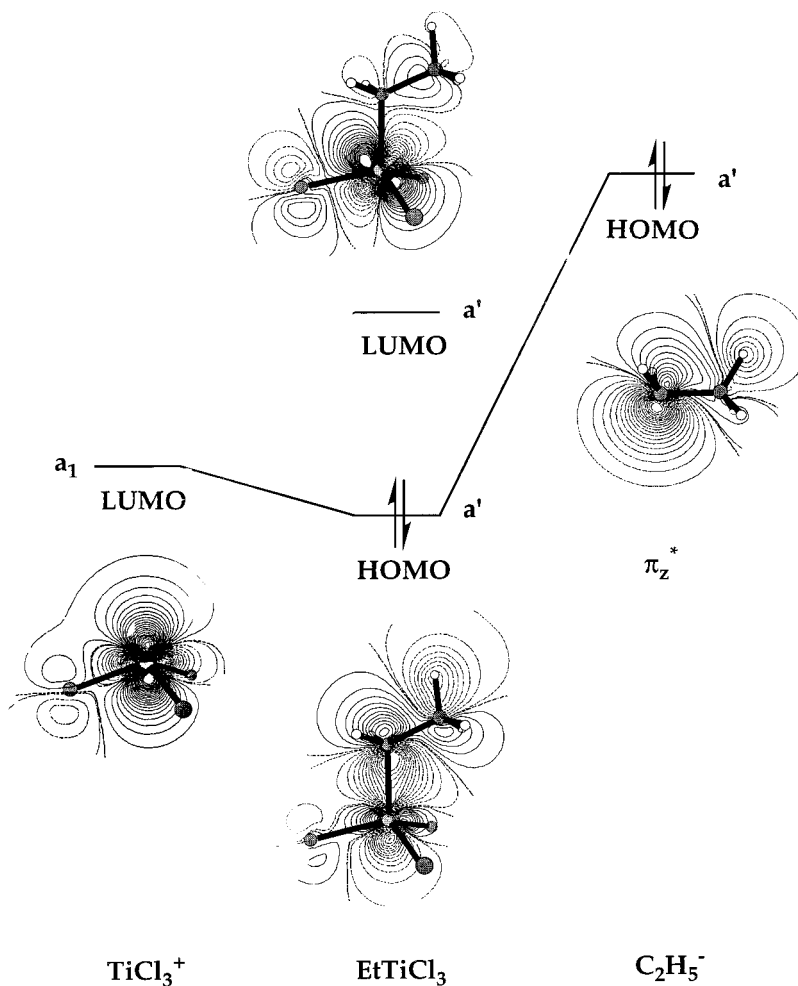


**Figure 2.** Frontier orbital interaction diagram and constant probability density contours for EtTiCl<sub>3</sub> (**1**).

coordination geometry of the metal to be distorted octahedral with the entire ethyl group occupying one coordination site; Table 1 lists the structural parameters. Most remarkable is the TiCC valence angle of  $84.57(9)^\circ$ , a value close to the  $86.3(6)^\circ$  determined originally for a crystal at room temperature.<sup>14</sup> At  $150.1(2) \text{ pm}$ , the C–C bond distance within the ethyl group

appears more or less normal;<sup>15</sup> the earlier study<sup>14</sup> had reported a rather shorter distance [ $146.7(15) \text{ pm}$ ] suggestive of partial

(15) Statistical analysis of the C–C bond distances in transition metal ethyl compounds based on 107 X-ray structures in the Cambridge Structural Database 5.10 (ref 7a) yields an average of  $147.5 \text{ pm}$ . These bond distances may, however, suffer from systematic shortening due to polarisation effects.

olefinic character. Electron density maps are in agreement with the eclipsed conformation of the ethyl group and identify a curiously short  $\text{Ti}\cdots\text{H}_\beta$  distance of about 206(2) pm. No less remarkable, though, is the  $\text{Ti}\cdots\text{C}_\beta$  distance, 250.1(2) pm, which is only 17% longer than the bonded  $\text{Ti}-\text{C}_\alpha$  distance.

The IR spectra of **2** in its normal and specifically deuterated forms reveal an unusually low stretching frequency for the unique in-plane  $\text{C}_\beta\text{-H}'$  bond.<sup>6</sup> Thus, the isotopomer  $\text{CHD}_2\text{CD}_2\text{-TiCl}_3(\text{dmpe})$  (**2-h1**) gives an "isolated" mode,  $\nu^{\text{is}}(\text{CH})$ ,<sup>16</sup> with a frequency of 2585  $\text{cm}^{-1}$ . This is some 200  $\text{cm}^{-1}$  lower than that of any  $\nu^{\text{is}}(\text{CH})$  mode reported hitherto (cf. 2799  $\text{cm}^{-1}$  in  $\text{NMe}_3$  where the C-H bonds are weakened through interaction with the antiperiplanar lone pair<sup>16</sup>). At the same time, the  $\nu$ -(CH) modes associated with the methylene portion of the ethyl ligand in **1** suffer a significant increase in frequency on coordination by dmpe [from 2878, 2933  $\text{cm}^{-1}$  in **1** to 2933, 3028  $\text{cm}^{-1}$  in **2**].<sup>6</sup> Hence it appears that complexation results in an appreciable weakening of the in-plane  $\text{C}_\beta\text{-H}'$  bond and a strengthening of the  $\text{C}_\alpha\text{-H}$  bonds as well as a widening of the  $\text{HC}_\alpha\text{H}$  angle. To facilitate the interpretation of the vibrational spectra of **2** in its different isotopic guises, we optimized also the molecular structure of the model compound  $\text{EtTiCl}_3(\text{dhpe})$  (**2a**; dhpe =  $\text{H}_2\text{PCH}_2\text{CH}_2\text{PH}_2$ ), with the ethyl group in an eclipsed conformation, and calculated the molecular force field and vibrational frequencies. The optimized structure was very similar to the calculated and experimentally determined structures found for **2** (see Table 1), so that the methyl groups on the P atoms appear to have very little effect on the overall structure of the complex. Hence the calculated harmonic frequencies of the eclipsed conformer of **2a** may be used with some confidence to aid the assignment of the IR spectrum of **2**<sup>6</sup> and indeed reproduce the principal  $\nu(\text{CH})$  features of the measured spectrum remarkably well (see Supporting Information).

Empirical equations described elsewhere<sup>16</sup> point (i) to an in-plane  $\text{C}_\beta\text{-H}'$  bond in **2** 3.6 pm longer and with a dissociation enthalpy 31  $\text{kcal mol}^{-1}$  smaller than its out-of-plane ( $\text{C}_\beta\text{-H}''$ ) counterparts and (ii) to  $\text{C}_\alpha\text{-H}$  bonds roughly 1.3 pm shorter and 5  $\text{kcal mol}^{-1}$  stronger than those in **1**.<sup>6</sup> Inspection of the calculated force field reveals the normal mode characterizing the  $\text{C}_\beta\text{-H}$  stretching vibration to consist exclusively of a rectilinear motion almost perpendicular to the  $\text{Ti-H}$  directrix and thus vitiates against description of the  $\beta$ -agostic interaction in terms of a  $\text{C}_\beta\text{-H-M}$  bridging bond.

The  $^{13}\text{C}$  NMR spectra of **1** and **2**<sup>14</sup> in  $\text{CD}_2\text{Cl}_2$  solution show that, as expected, coordination by dmpe shifts both the  $\text{C}_\alpha$  and  $\text{C}_\beta$  resonances to lower frequency, whereas  $J_{\text{CH}}$  for the  $\text{C}_\beta\text{H}_3$  unit decreases somewhat (from an averaged value of 130.0 to 125.7 Hz), and  $J_{\text{CH}}$  for the  $\text{C}_\alpha\text{H}_2$  unit increases significantly (from 134.3 to 147.3 Hz). The last value is in accord with the corresponding parameter reported for other  $\beta$ -agostic ethyl complexes<sup>8a,b,9a</sup> and also, notably, for cyclopropane (161 Hz);<sup>9a</sup> it is consistent too with the IR properties described above.  $^1\text{H}$  NMR studies have also been carried out on  $\text{CDH}_2\text{CH}_2\text{TiCl}_3$  (**1-d1**) and its dmpe adduct **2-d1**, appealing to the isotopic perturbation of resonance (IPR) method of Shapley et al.<sup>17,18</sup> for evidence of  $\text{Ti}\cdots\text{H}$  interactions. **1** displays an isotope shift

(16) See, for example: McKean, D. C. *Chem. Soc. Rev.* **1978**, 7, 399–422; *Croat. Chem. Acta* **1988**, 61, 447–461; *Int. J. Chem. Kinet.* **1989**, 21, 445–464.

(17) (a) Saunders, M.; Telkowski, L.; Kates, M. R. *J. Am. Chem. Soc.* **1977**, 99, 8070–8071. (b) Calvert, R. B.; Shapley, J. R. *J. Am. Chem. Soc.* **1978**, 100, 7726–7727.

(18) Hansen, P. E. *Annu. Rep. NMR Spectrosc.* **1983**, 15, 105–234; Harris, R. K. *Nuclear Magnetic Resonance Spectroscopy*; Longman: London, 1986; p 194.

**Table 3.** Experimental and Calculated (DFT-GIAO)  $^{13}\text{C}$  Chemical Shifts  $\delta$  (in ppm Relative to TMS) for  $\text{Me}_2\text{TiCl}_2$ ,  $\text{MeTiCl}_3$ ,  $\text{EtTiCl}_3$  (**1**), and  $\text{EtTiCl}_3(\text{dmpe})$  (**2**)

molecule	nucleus	$\delta$ (exp) <sup>a</sup>	$\delta$ (calc) <sup>b</sup>
$\text{Me}_2\text{TiCl}_2$ <sup>b</sup>	$\text{C}_\alpha$	99.6	82.6
$\text{MeTiCl}_3$ <sup>b</sup>	$\text{C}_\alpha$	118.2	93.2
$\text{EtTiCl}_3$ <sup>b</sup>	$\text{C}_\alpha$	139.65	117.7
	$\text{C}_\beta$	21.35	26.5
$\text{EtTiCl}_3(\text{dmpe})$ <sup>c</sup>		$T = 213 \text{ K} / T = 273 \text{ K}$	ecl/stag
	$\text{C}_\alpha$	81.04/85.16	69.2/83.4
	$\text{C}_\beta$	3.81/5.76	5.6/11.1
	$\text{PCH}_2$	27.77/28.11	34.3/34.1
	$\text{PCH}_2$	23.08/23.58	30.1/30.1
	$\text{PCH}_3$ <sup>d</sup>	14.05/13.91	19.2/19.6
	$\text{PCH}_3$ <sup>d</sup>	13.80/13.91	18.0/17.2

<sup>a</sup> All experimental shifts in  $\text{CD}_2\text{Cl}_2$  solution. <sup>b</sup> This work: experimental values measured at 243 K. <sup>c</sup> Reference 14. <sup>d</sup> Averaged values.

$\Delta = [\delta(\text{CH}_3) - \delta(\text{CH}_2\text{D})]$  of about 0.019 which varies slightly with temperature. By contrast, **2** has an isotope shift varying between  $-0.05$  and  $-0.01$  in the temperature range 193–313 K; the magnitude and temperature-dependence of the IPR are both small, but, to our knowledge, this is the first example of a molecule with a negative IPR.<sup>19</sup>

Structure optimization of **2** was carried out by DFT calculations without the imposition of symmetry constraints. The global energy minimum was found for a  $\text{TiC}_\alpha\text{C}_\beta$  angle of 85.5° and an eclipsed ethyl group conformation. Comparison with the structure parameters determined by X-ray crystallography reveals good agreement between theory and experiment (see Table 1). The strength of the agostic interaction may be estimated from the calculations by subtracting the energy of the agostic equilibrium structure from the energy of an optimized model with a staggered conformation and the  $\text{TiC}_\alpha\text{C}_\beta$  valence angle fixed at 112°: this gives a stabilization energy, to be denoted  $D_{112}$ , of 1.84  $\text{kcal mol}^{-1}$ .<sup>20b,c</sup>

A more extensive search of the potential energy surface led to the identification of another local energy minimum corresponding to a second conformer which is also agostic, being characterized by a  $\text{TiC}_\alpha\text{C}_\beta$  angle of 93.1° and a staggered ethyl group conformation. This conformer is calculated to lie only 0.18  $\text{kcal mol}^{-1}$  above the equilibrium structure and 1.66  $\text{kcal mol}^{-1}$  below the optimized agostic model with  $\angle\text{TiC}_\alpha\text{C}_\beta = 112^\circ$ . The energy difference between the two agostic conformers is so small that their relative stabilities cannot be regarded as established on the basis of the DFT calculations alone, and the structure adopted in the crystal may well be determined in the final analysis by intermolecular forces. The crucial conclusion to emerge from the calculations is that *agostic interactions do not necessarily require an ethyl group in which a  $\text{C}_\beta\text{-H}$  bond points toward the metal atom.* We shall return to this point subsequently.

In Table 3 we compare the  $^{13}\text{C}$  chemical shifts of  $\text{Me}_2\text{TiCl}_2$ ,  $\text{MeTiCl}_3$ ,  $\text{EtTiCl}_3$ , and  $\text{EtTiCl}_3(\text{dmpe})$  calculated at the DFT-

(19) Green, M. L. H.; Hughes, A. K.; Popham, N. A.; Stephens, A. H. H.; Wong, L.-L. *J. Chem. Soc., Dalton Trans.* **1992**, 3077–3082. For an alternative explanation of the observed IPR see: Maus, D. C.; Copié, V.; Sun, B.; Griffiths, J. M.; Griffin, R. G.; Luo, S.; Schrock, R. R.; Liu, A. H.; Seidel, S. W.; Davis, W. M.; Grohmann, A. *J. Am. Chem. Soc.* **1996**, 118, 5665–5671.

(20) Higher stabilization energies were found for the model systems  $\text{EtTiCl}_2\text{H}(\text{PH}_3)_2$  and  $\text{EtTiCl}_3(\text{PH}_3)_2$  on the basis of SCF and LDF-DFT calculations. For further information, see: (a) Endo, J.; Koga, N.; Morokuma, K. *Organometallics* **1993**, 12, 2777–2787. (b) Munakata, H.; Ebisawa, Y.; Takashima, Y.; Wrinn, M. C.; Scheiner, A. C.; Newsam, J. M. *Catal. Today* **1995**, 23, 402–408. (c) Koga, N.; Obara, S.; Morokuma, K. *J. Am. Chem. Soc.* **1984**, 106, 4625–4626.

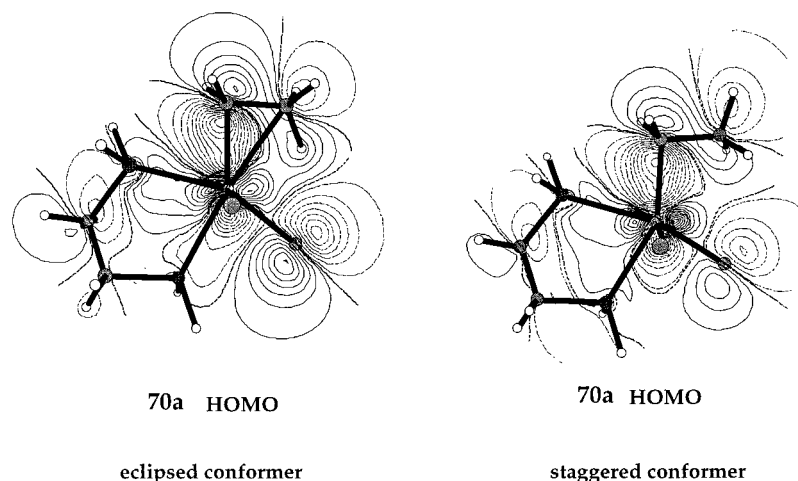


**Figure 3.** Constant probability density contours of the HOMO's of the eclipsed and staggered conformers of  $\text{EtTiCl}_3(\text{dhpe})$  (**2a**).

GIAO level with the experimental results. Despite the lack of quantitative agreement between theory and experiment<sup>21</sup> (in the case of  $\text{MeTiCl}_3$  the values differ by 25 ppm), the calculations successfully reproduce the monotonic increase of  $C_\alpha$  shifts observed for the series



They also reproduce the large difference in chemical shift between  $C_\alpha$  and  $C_\beta$  in  $\text{EtTiCl}_3$  as well as the increased shielding of both carbon atoms on coordination with dmpe. We have some confidence therefore in the ability of the calculations to estimate the *difference* between the chemical shifts of the  $C_\alpha$  and  $C_\beta$  nuclei in the eclipsed and staggered conformers of **2**. On the evidence of the calculations, both  $C_\alpha$  and  $C_\beta$  resonate at lower frequency in the eclipsed conformer of **2**, a result of some significance since the experimental  $C_\alpha$  and  $C_\beta$  resonances both move to lower frequency as the temperature decreases. Green *et al.*<sup>14</sup> noted this temperature dependence and suggested an equilibrium between the structure deduced by X-ray crystallography and another conformer in which the ethyl group has been rotated through  $90^\circ$  into a plane normal to that defined by the  $\text{TiP}_2$  geometry. We have attempted to optimize the structure of such a conformer and find that it converges to the observed geometry. Hence we propose that the temperature variation in the chemical shifts arises from an equilibrium between staggered and eclipsed conformers, with the latter being the more stable. The measured NMR spectra are in keeping therefore with the greater stability of the eclipsed conformer and with the thermal accessibility of the staggered conformer predicted by the DFT calculations.

A possible explanation for the negative IPR revealed by the  $^1\text{H}$  NMR spectra of **2** and **2-d**<sub>1</sub> is that the agostic H atom of the  $\text{CH}_3$  group ( $C_\beta\text{-H}'$ ) is not more but *less* shielded than the anagostic ones ( $C_\beta\text{-H}''$ ). This proposal is in contrast with the original assumption that agostic hydrogen atoms always display a low-frequency shift.<sup>22</sup> It accords, however, with the results of calculations at the DFT-GIAO level, which yield  $^1\text{H}$  chemical shifts of 3.63 ppm for the agostic and 1.51/1.45 ppm for the anagostic H atoms on the  $\beta$ -carbon atom, and also with the vibrational properties deduced for the  $C_\beta\text{-H}'$  bond. The magnitude of the Shapley effect (i.e., the temperature depen-

dence of the IPR) may be expected also to be reduced by the presence of the staggered conformer with calculated  $C_\beta\text{H}_3$  shifts of 1.80, 1.92, and 2.21 ppm (see the table in the Supporting Information for further information about the calculated  $^1\text{H}$  shifts in **1** and **2**). We conclude then that the results of the Shapley experiment as applied to **2** may not prove, but are wholly accordant with, the *deshielding* of the agostic H atom in **2** foretold by the DFT-GIAO calculations.

Constant electron density contours of the HOMO of eclipsed and staggered conformers of **2a** are depicted in Figure 3. Comparison with the HOMO of the anagostic compound **1** (Figure 2) is instructive: both HOMO's may be described as  $\text{Ti-C}_\alpha$  bonding orbitals, but the ethyl group in the dhpe adduct has been canted in such a way that there is now positive overlap between the torus of the Ti  $d_{z^2}$  atomic orbital and the  $C_\beta\text{H}'$  fragment. In addition, though, there is an antibonding interaction between Ti and the in-plane Cl(1) atom which may facilitate the distortion of the coordination geometry of the metal accompanying the reduction of the  $\text{TiC}_\alpha\text{C}_\beta$  angle.

We turn next to the results of further DFT calculations carried out on a variety of model ethyl-transition metal compounds with the aim of probing the effects of varying the net charge, the nature, or the coordination number of the metal atom.

**2.4. DFT Calculations on  $[\text{EtTiCl}_2]^+$  (**3**): Strong Agostic Interactions.** Structure optimization of a model of the cation  $[\text{EtTiCl}_2]^+$  (**3**) with  $C_s$  symmetry and an eclipsed ethyl group conformation yielded an acute MCC angle of  $85.0^\circ$  and a short  $\text{Ti}\cdots\text{H}_\beta$  distance of 206 pm. Calculation of the molecular force field yielded no imaginary frequencies, showing that the eclipsed conformer corresponds to a minimum on the global potential energy surface. The  $\beta$ -agostic stabilization energy, estimated by comparison with an optimized model in which the  $\text{TiCC}$  angle has been fixed at  $112^\circ$ , is  $8.36 \text{ kcal mol}^{-1}$ . In the following discussion we shall classify an agostic interaction as strong if the interaction energy is larger than  $5 \text{ kcal mol}^{-1}$ .

Optimization of a  $C_s$  model with a staggered ethyl group conformation yielded an even more acute  $\text{TiCC}$  valence angle of  $80.0^\circ$ . The energy of this model is  $0.68 \text{ kcal mol}^{-1}$  above that of the eclipsed conformer and  $7.68 \text{ kcal mol}^{-1}$  below that of the optimized, nonagostic model with  $\angle\text{TiCC} = 112^\circ$ .<sup>23</sup> As in the case of  $\text{EtTiCl}_3(\text{dmpe})$ , we find that the agostic stabilization energy of a model with a staggered ethyl group is only

(21) The large methyl  $^{13}\text{C}$  shift of 83.1 ppm observed for  $\text{W}(\text{CH}_3)_6$  was also underestimated by DFT calculations (62 ppm). For further information see Kaupp, M. *J. Am. Chem. Soc.* **1996**, *118*, 3018–3024.

(22) Emsley, J. W.; Feeney, J.; Sutcliffe, L. H. *High-Resolution NMR Spectroscopy*; Pergamon: Oxford, 1966. Vol. 2, pp 825–826.

(23) (a) Woo *et al.* have published the results of high-quality DFT calculations on  $[(n\text{-propyl})\text{ZrCp}_2]^+$  that indicate the existence of a  $\gamma$ -agostic conformer where two  $\text{H}_\gamma$  atoms are about equally far from the metal atom (ref 4b). (b) Fan *et al.* have computed the equilibrium structure of  $[\text{EtTiCl}_2]^+$

**Table 4.** Salient Structural Parameters of the Model System  $[\text{EtTiCl}_2]^+$  (**3**)<sup>a</sup>

parameter	$[\text{EtTiCl}_2]^+$ ecl <sup>b</sup>	$[\text{EtTiCl}_2]^+$ stag <sup>b</sup>	$[\text{EtTiCl}_2]^+$ stag <sup>b/112</sup> <sup>c</sup>
$\Delta E_{\text{rel}}$	0	0.68	8.36
$N_{\text{imag}}$	0	1	
$\angle \text{MCC}$	85.0	80.0	112.0
M—C	201.4	199.9	200.5
C—C	152.1	154.4	153.5
$\text{C}_\beta\text{—H}'$ <sup>c</sup>	115.4	110.3	110.4
$\text{C}_\beta\text{—H}''$ <sup>c</sup>	109.7	111.4	110.1
M—Cl	215.0	215.0	214.8
$\angle \text{MCH}$	113.0	116.2	105.9
$\angle \text{CCH}_\beta'$ <sup>c</sup>	114.5	109.8	107.6
$\angle \text{CCH}_\beta''$ <sup>c</sup>	113.6	114.6	113.5
$\angle \text{CIMCl}$	116.1	114.8	111.3
$\angle \text{CMCl}$	109.0	108.8	108.1
$\text{M}\cdots\text{H}_\beta$ <sup>d</sup>	206.0	243.8	319.2
$\text{M}\cdots\text{C}_\beta$	241.7	230.3	294.6

<sup>a</sup> Bond distances in pm, angles in deg, and energies in kcal mol<sup>-1</sup>.  $N_{\text{imag}}$  = number of imaginary frequencies. <sup>b</sup> The labels "ecl" and "stag" specify the ethyl group conformation. The value of 112° relates to the TiCC angle. <sup>c</sup> Atom in the symmetry plane is denoted by ('); atom out of the symmetry plane is denoted by ("). <sup>d</sup> Shortest Ti⋯H<sub>β</sub> distance.

about 10% lower than for an eclipsed model. We assume that, in general, the conformation adopted by an ethyl group bonded to a transition metal atom will be determined by the balance of two opposing forces: (i) the inherent barrier to rotation about the C—C bond which favors a staggered conformation and (ii) the strength of the β-agostic interaction which favors an eclipsed conformation.

For EtTiCl<sub>3</sub>(dmpe) the staggered model corresponds to a local minimum on the potential energy surface. In the case of  $[\text{EtTiCl}_2]^+$ , calculation of the molecular force field shows that the staggered model corresponds to a transition state for internal rotation of the methyl group. In summary, the calculations yield a barrier to internal rotation of the methyl group of 0.68 kcal mol<sup>-1</sup> and indicate that rotation occurs with only a small change of TiCC angle. Such "in-place" rotation of a methyl group involved in a β-agostic interaction has been inferred from NMR measurements in at least one case.<sup>24</sup>

Optimized structure parameters for both the eclipsed equilibrium structure and for the staggered transition state of **3** are listed in Table 4.

**2.5. The Nature of β-Agostic Interactions in Ethyl Derivatives of Early Transition Metals.** We now turn our attention to the bonding between the transition metal atom and the β-agostic ethyl group. In Figure 4 we display constant-probability-density contours in the TiCC plane as well as a three-dimensional constant probability surface of the HOMO for the eclipsed equilibrium structure of  $[\text{EtTiCl}_2]^+$ . The nature of the HOMO is clearly similar to that of EtTiCl<sub>3</sub>(dhpe) (see Figure 3), but the smaller number of ligands and the higher symmetry (*C<sub>s</sub>* versus *C<sub>1</sub>*) cause the HOMO now to be localized on the EtTi fragment. For this reason, and since the agostic interaction is strong, we prefer to base our discussion of the nature of β-agostic interactions on the case of  $[\text{EtTiCl}_2]^+$ .

Comparison of  $[\text{EtTiCl}_2]^+$  with the anagostic compound EtTiCl<sub>3</sub> (Figure 2) shows that the HOMO's of both may be described as Ti—C<sub>α</sub> σ-bonding orbitals formed by combination of the metal-based d<sub>z<sup>2</sup></sub> atomic orbital (with a small admixture

and report parameters in good agreement with ours: Fan, L.; Harrison, D.; Deng, L.; Woo, T. K.; Swerhone, D.; Ziegler, T. *Can. J. Chem.* **1995**, *73*, 989–998. These studies explored neither the potential surface around the equilibrium geometry nor the nature of the bonding therein.

(24) Derome, A. E.; Green, M. L. H.; Wong, L.-L. *New J. Chem.* **1989**, *13*, 747–753.

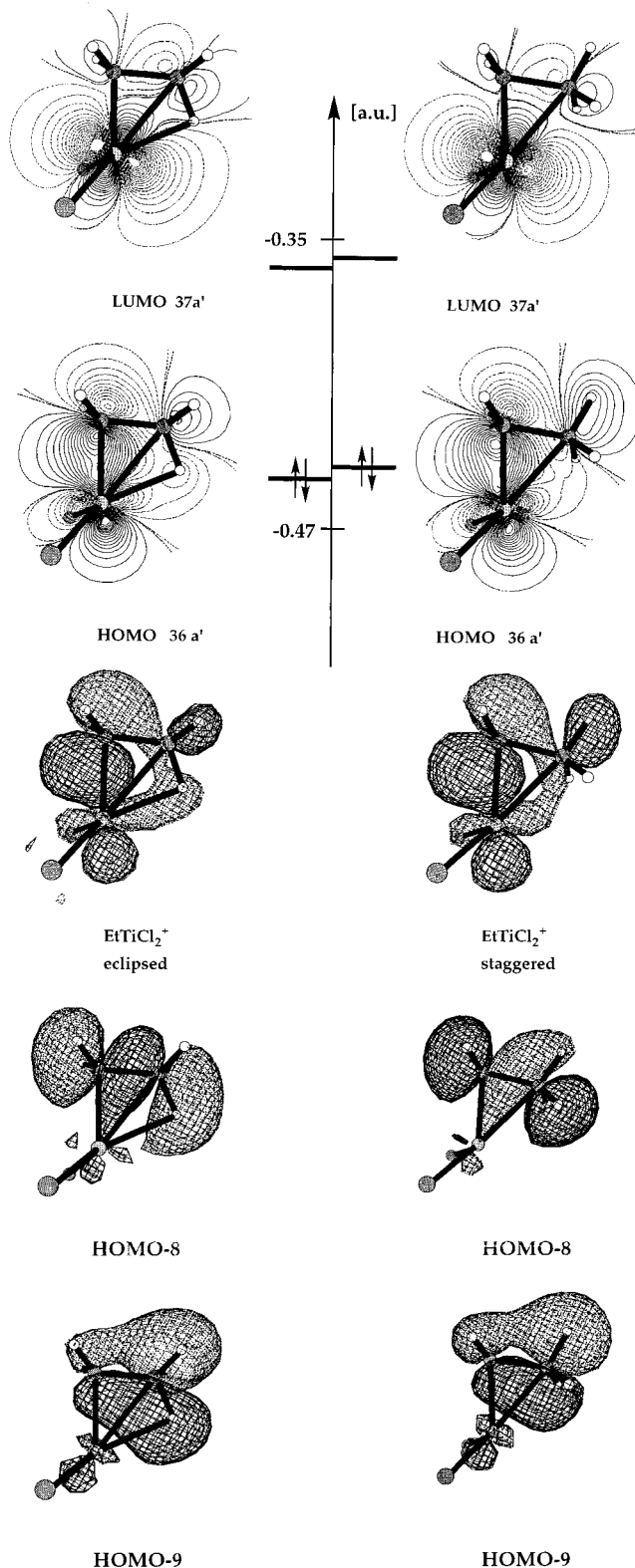


**Figure 4.** Top: constant probability density contours in the TiCC plane of the HOMO and LUMO of  $[\text{EtTiCl}_2]^+$  (**3**). Bottom: three-dimensional constant probability density surfaces of the HOMO, HOMO-8, and HOMO-9 orbitals.

of s and p functions) with the C—H bonding but C—C antibonding  $\pi_z^*$  orbital of the ethyl fragment. As in **2a**, however, the ethyl group in  $[\text{EtTiCl}_2]^+$  has been canted in such a way that there is now a positive overlap between the torus of the Ti d<sub>z<sup>2</sup></sub> orbital and the C<sub>β</sub>H' fragment. At the same time, comparison of orbital energies shows that the HOMO in **3** is

stabilized by 6.5 kcal mol<sup>-1</sup> when the TiCC angle is reduced from 112 to 85°. We suggest therefore that the  $\beta$ -agostic interaction should be regarded as a covalent interaction which can be understood only in terms of a Ti–C $_{\alpha}$  bonding orbital that is delocalized *over the entire ethyl group*: the reduction of the MCC valence angle allows the metal atom to establish bonding interactions with the  $\beta$ -C and its appended H atom. The geometry of the M–Et interaction is such that bonding to both C $_{\alpha}$  and C $_{\beta}$  is effected by the *same* orbital on M. Such a situation is well established for other transition-metal–C<sub>2</sub> ligand interactions, the classic example being the Dewar–Chatt–Duncanson description of M–olefin bonding.<sup>25</sup>

Comparison of orbital energies shows that reduction of the TiCC angle also leads to significant stabilization of two deeper lying MO's, viz. the HOMO-8 and HOMO-9 orbitals. Three-dimensional constant-probability-density surfaces (Figure 4) show that the former is a C–C  $\sigma$ -bonding orbital, while the latter is a delocalized C–H bonding orbital. Both orbitals appear to be slightly delocalized onto the metal atom. The delocalization is, however, so small that a  $\beta$ -agostic alkyl group may still be considered a two-electron ligand.<sup>26</sup>

Mulliken population parameters of the orbitals obtained by calculations on an anagostic structure (i.e., with  $\angle$ TiCC greater than 112°) suggest that the ethyl group carries a net negative charge. When the MCC angle is closed, there appears to be a slight depolarization of Et–Ti bonding, with a small amount of negative charge being returned to the metal atom. The bond distances and valence angles listed in Table 4 indicate that establishment of agostic interactions leads to a small reduction of the C–C bond distance, a slight increase of the in-plane C–H' bond distance, and an opening of the CCH' angle in the eclipsed conformer. These structural changes are consistent with depopulation of the  $\pi_z^*$  ligand orbital.

Figure 4 also shows constant-probability-density contour plots for the HOMO of the transition state to methyl group rotation. These suggest that rotation of the methyl group into a staggered position eliminates the bonding interactions between the metal atom and  $\beta$ -hydrogen atoms; the H atoms that are now closest to Ti are situated near a nodal surface. We suggest, therefore, that the stabilization of the small TiCC angle is best described as an agostic Ti $\cdots$ C $_{\beta}$ , rather than a Ti $\cdots$ H<sub>2</sub>C $_{\beta}$  interaction. The fact that the strength of the agostic interaction increases by less than 10% on rotation of the methyl group from a staggered to an eclipsed conformation implies that in the eclipsed conformation *too the main contribution to the  $\beta$ -agostic stabilization energy derives from Ti $\cdots$ C $_{\beta}$  bonding*. In this context, it may be remarked, Mulliken population analyses on Et–M compounds consistently indicate that, as expected, the metal atom and all H atoms carry net positive charges, while the C atoms carry net negative charges. The agostic interaction could therefore be enhanced by Coulomb attraction between the M and C $_{\beta}$  atoms and opposed by Coulomb repulsion between M and H $_{\beta}$  atoms. Coulomb attraction between M and C $_{\beta}$  provides a possible rationalization of the apparent strengthening of the agostic effect in complexes such as **3** carrying a net positive charge.

Within the agostic molecule the maximum electron density in the TiC $_{\alpha}$  bonding region is no longer found on the Ti–C $_{\alpha}$  directrix; instead the bond appears to be “bent”. We suggest that this bending is a consequence of canting of the ethyl group;

the C–C bond distance is too short to allow optimal interaction of Ti with both carbon atoms of the ethyl group.

**2.6. DFT Calculations on EtScCl<sub>2</sub> (4) and EtTiCl<sub>2</sub> (5): Weak Agostic Interactions.** Structure optimizations of **4** and **5** indicate that the equilibrium structures have eclipsed ethyl group conformations, acute MCC angles of 86.5 and 85.6°, and short M $\cdots$ C $_{\beta}$  distances of 255 and 247 pm, respectively (see Supporting Information). The strength of the  $\beta$ -agostic interactions, estimated by comparison with optimized models with  $\angle$ MCC fixed at 112°, is 2.85 kcal mol<sup>-1</sup> for **4** and 0.99 kcal mol<sup>-1</sup> for **5**. Accordingly we classify both interactions as weak.

Optimization of a staggered model of **4** yields an ScCC angle of 83.5° and an imaginary methyl torsion frequency indicating a transition state; as in the case of [EtTiCl<sub>2</sub>]<sup>+</sup>, internal rotation of the methyl group occurs without rupture of the agostic interaction. The calculated barrier to methyl group rotation is 0.95 kcal mol<sup>-1</sup>. Optimization of a staggered model of **5** yields a TiCC angle of 107.5° indicating that the agostic interaction has been broken. Inspection of the methyl group rotation mode shows that the staggered model corresponds to a local minimum on the potential energy surface, i.e., to a higher energy conformer. Since the energy difference, 0.98 kcal mol<sup>-1</sup>, is comparable with the thermal energy available at room temperature (RT = 0.6 kcal mol<sup>-1</sup>), both conformers may coexist in the gas phase or in solution in a weakly interacting solvent.<sup>27</sup>

EtScCl<sub>2</sub> is related to the complex EtScCp\*<sub>2</sub> and EtTiCl<sub>2</sub> to EtTiCp\*<sub>2</sub> through the isolobality of the Cp\* group and the Cl atom.<sup>28</sup> As mentioned in section 2.1, there is strong spectroscopic and kinetic evidence for  $\beta$ -agostic interactions in both Cp\* compounds.<sup>9,10</sup> Lukens et al. have assigned separate electronic absorptions of EtTiCp\*<sub>2</sub> in hydrocarbon solution to agostic and anagostic conformers. The temperature variation of the intensities yielded an estimated energy difference of 1.9 kcal mol<sup>-1</sup>.<sup>10b</sup> The properties calculated for the model compound EtTiCl<sub>2</sub> are thus in good agreement with those estimated experimentally for EtTiCp\*<sub>2</sub>.

Geometric rearrangement of an ethyl ligand to allow establishment of  $\beta$ -agostic interaction requires additional space in the coordination sphere of the metal atom. The rearrangement may therefore be opposed by interligand repulsion. This is hardly a problem in three-coordinate species such as **3**, **4**, or **5**, since the orientation of the ethyl group is such that the MC $_{\alpha}$ C $_{\beta}$  and MCl<sub>2</sub> planes are perpendicular. As a result, the shortest Cl $\cdots$ C $_{\beta}$  distance in [EtTiCl<sub>2</sub>]<sup>+</sup> is 399 pm, as compared to 383 pm (by DFT calculations) in the nonagostic molecule EtTiCl<sub>3</sub>. In the same vein, one would not expect serious strain in the pentamethylcyclopentadienyl analogue [EtTiCp\*<sub>2</sub>]<sup>+</sup> since the agostic ethyl group could occupy the cleft between the nonparallel Cp\* rings.

**2.7. DFT Calculations on the Four-Coordinate Model Compounds EtZrCl<sub>3</sub> (6), EtVCl<sub>3</sub> (7), EtNbCl<sub>3</sub> (8), and [EtVCl<sub>3</sub>]<sup>+</sup> (9): Repulsion between Ligands and a Rigid Coordination Geometry May Obstruct  $\beta$ -Agostic Interactions Even with a Net Positive Charge on the Metal.** We have seen (section 2.2) that it requires no more than 2.8 kcal mol<sup>-1</sup> to reduce the TiCC angle in EtTiCl<sub>3</sub> from 115 to 95°. We have also seen (sections 2.4 and 2.6) that the agostic interaction in the cationic complex [EtTiCl<sub>2</sub>]<sup>+</sup> is some 5.5 kcal

(27) The potential energy curve calculated for staggered EtTiCl<sub>2</sub> is extremely flat, and so we should add two cautionary notes. First, even small changes in the computational approach could have a large effect on the optimal value of the TiCC angle. Second, the shape of the barrier to methyl group rotation might be significantly changed, particularly in the range from  $\tau = 40$  to 60°.

(28) (a) Reference 2, pp 396–401. (b) Hoffmann, R. *Angew. Chem., Int. Ed. Engl.* **1982**, *21*, 711–724.

(25) Reference 2, pp 259–260.

(26) Eisenstein and co-workers have also suggested a two-electron description of  $\beta$ -agostic interactions on the basis of extended Hückel calculations on the species [EtTiH<sub>5</sub>]<sup>2-</sup>: Demolliens, A.; Jean, Y.; Eisenstein, O. *Organometallics* **1986**, *5*, 1457–1464.



**Table 5.** Salient Structural Parameters of the Model Systems EtTiCl<sub>3</sub> (**1**), EtZrCl<sub>3</sub> (**6**), EtVCl<sub>3</sub> (**7**), EtNbCl<sub>3</sub> (**8**), and [EtVCl<sub>3</sub>]<sup>+</sup> (**9**)<sup>a</sup>

parameter	EtTiCl <sub>3</sub> stag <sup>b</sup>	EtTiCl <sub>3</sub> ecl <sup>b</sup>	EtZrCl <sub>3</sub> stag <sup>b</sup>	EtZrCl <sub>3</sub> ecl <sup>b</sup>	EtVCl <sub>3</sub> <sup>e</sup> stag <sup>b</sup>	EtVCl <sub>3</sub> <sup>e</sup> ecl <sup>b</sup>	EtNbCl <sub>3</sub> ecl <sup>b</sup>	EtNbCl <sub>3</sub> stag <sup>b</sup>	[EtVCl <sub>3</sub> ] <sup>+</sup> stag <sup>b</sup>	[EtVCl <sub>3</sub> ] <sup>+</sup> ecl <sup>b</sup>
$\Delta E_{\text{rel}}$	0	1.71	0	0.98	0	0.76	0	0.55	0	1.57
$N_{\text{imag}}$	0	1	0	1	0	0	0	1	0	1
$\angle \text{MCC}$	117.2	112.3	112.2	99.7	111.2	91.1	91.9	106.1	117.4	110.4
M–C	205.2	204.7	217.5	216.6	201.5	199.7	210.4	211.5	197.2	196.8
C–C	153.0	153.9	155.6	156.1	153.1	152.6	155.5	155.9	152.1	153.1
C–H <sub><math>\beta</math>'</sub> <sup>c</sup>	110.3	110.3	110.6	111.9	110.4	112.1	112.8	110.6	110.4	110.4
C–H <sub><math>\beta</math>''</sub> <sup>c</sup>	109.9	110.4	110.4	110.1	109.8 <sup>e</sup>	109.8 <sup>e</sup>	110.0	110.3	109.8	109.8
M–Cl' <sup>c</sup>	220.7	220.5	238.9	238.7	216.1	216.5	234.8	234.6	209.8	209.5
M–Cl'' <sup>c</sup>	220.6	220.9	239.2	239.9	217.2 <sup>e</sup>	218.8 <sup>e</sup>	237.5	236.4	209.5	209.9
$\angle \text{MCH}$	103.3	104.8	107.3	111.4	105.9	111.4	113.5	110.0	100.4	102.8
$\angle \text{CC}_{\beta}\text{H}'$ <sup>c</sup>	110.6	113.9	110.5	114.5	109.6	114.1	114.8	109.3	107.6	115.0
$\angle \text{CC}_{\beta}\text{H}''$ <sup>c</sup>	111.9	111.1	111.8	111.2	112.3 <sup>e</sup>	112.1 <sup>e</sup>	111.4	112.2	112.6	109.9
$\angle \text{Cl}'\text{MCl}''$ <sup>c</sup>	113.4	114.4	115.1	117.7	110.1	113.7	111.5	108.6	112.0	113.6
$\angle \text{Cl}'\text{MCl}'$ <sup>c</sup>	113.0	112.2	112.9	110.5	114.1 <sup>e</sup>	109.1 <sup>e</sup>	112.1	115.8	112.0	110.7
$\angle \text{CMCl}'$ <sup>c</sup>	105.3	105.3	104.7	105.1	102.3	98.6	97.9	99.7	107.0	106.4
$\angle \text{CMCl}''$ <sup>c</sup>	105.6	105.9	105.0	106.0	107.9 <sup>e</sup>	112.6 <sup>e</sup>	111.2	108.1	106.7	107.5
M···H <sub><math>\beta</math>'</sub> <sup>d</sup>	329.1	289.9	329.7	263.7	314.3 <sup>e</sup>	224.2	236.0	312.2	324.9	281.4
M···C <sub><math>\beta</math></sub>	306.9	299.2	311.7	287.5	293.9	253.6	265.8	295.5	299.4	288.5

<sup>a</sup> Bond distances in pm, angles in deg, and energies in kcal mol<sup>-1</sup>.  $N_{\text{imag}}$  = number of imaginary frequencies. <sup>b</sup> The labels “ecl” and “stag” specify the ethyl group conformation. <sup>c</sup> Atom in the symmetry plane is denoted by ('); atom out of the symmetry plane is denoted by ("). <sup>d</sup> Shortest M···H <sub>$\beta$</sub>  distance. <sup>e</sup> Average values; geometry was optimized without symmetry constraints.

mol<sup>-1</sup> stronger than in the isoelectronic neutral complex EtScCl<sub>2</sub>. Expecting that an increase in the formal charge on the metal would have a similar effect in four-coordinated species, therefore, we carried out calculations on [EtVCl<sub>3</sub>]<sup>+</sup> (**9**). To our surprise, however, we found that the equilibrium structure is *anagostic* with  $\angle \text{VCC} = 117.4^\circ$  and a staggered ethyl group conformation. Optimization of a model in which the ethyl group is fixed in an eclipsed conformation yields  $\angle \text{VCC} = 110.4^\circ$  and an energy 1.57 kcal mol<sup>-1</sup> above that of the *anagostic* equilibrium structure. We conclude that *anagostic interaction is not invariably favored by a net positive charge on M*.

Structure optimization of **6** and **7** yields equilibrium structures similar to that obtained for the Ti analogue **1**; the valence angles ZrCC and VCC are slightly larger than tetrahedral and the ethyl group conformations staggered (see Table 5). Optimization of models in which ethyl groups are fixed in *eclipsed* conformations yield MCC angles of 99.7° (**6**) and 91.1° (**7**), as compared with 112.3° for the Ti analogue (**1**).<sup>29</sup> The energy of the optimized eclipsed conformer relative to that of the *anagostic* equilibrium structure decreases from 1.71 in **1** through 0.98 in **6** to 0.76 kcal mol<sup>-1</sup> in **7**. The optimized eclipsed models of **1** and **6** correspond to transition states for internal rotation of the methyl groups. The corresponding model for **7**, however, corresponds to a local minimum on the potential energy surface, indicating that gaseous EtVCl<sub>3</sub> may consist of a mixture of an *anagostic*, staggered and a less stable *agostic*, eclipsed conformer.<sup>30</sup>  $\beta$ -*Agostic* interactions in **6** and **7** may be described as incipient, since structures with MCC valence angles less than 100° and with eclipsed ethyl group conformations are thermally accessible at room temperature.

Finally, calculations on **8** yield a  $\beta$ -*agostic* equilibrium structure with  $\angle \text{NbCC} = 91.9^\circ$  and an eclipsed ethyl group. These results indicate that the stability of a  $\beta$ -*agostic* model relative to that of its *anagostic* counterpart increases in the order



We have suggested (see section 2.2) that the pliability of the TiCC valence angle in **1** is due to near-cancellation of *agostic* M···C <sub>$\beta$</sub> H attraction and steric C <sub>$\beta$</sub> H<sub>3</sub>···Cl'' repulsion. This repulsion should be reduced if a Fourth Period atom such as Ti or V is replaced by the larger Fifth Period congener Zr or Nb, and the *agostic* structure should become more stable. A referee suggested that we optimize the model system [EtZrCl<sub>2</sub>]<sup>+</sup> for comparison with [EtTiCl<sub>2</sub>]<sup>+</sup> in order to explore the effect of electronic differences between Fourth and Fifth Period elements. The interaction energy obtained for [EtZrCl<sub>2</sub>]<sup>+</sup>,  $D_{112} = 6.0$  kcal mol<sup>-1</sup>, is 1.0 kcal mol<sup>-1</sup> smaller than that calculated for the Ti analogue **3** (BPW91/II level), indicating that in these sterically unhindered systems the *agostic* interaction is, if anything, weaker in the Zr than in the Ti species. But why should *agostic* interactions be more favored in the Group 5 than in the Group 4 derivatives in these four-coordinated model systems? We believe that the answer may be sought partly in the nature of the HOMO which contains the additional electron and partly in the direction of the distortion which relieves C <sub>$\beta$</sub> H<sub>3</sub>···Cl'' repulsion (see Figure 5).

Examination of the *anagostic* equilibrium structure of EtVCl<sub>3</sub> shows that, while the three ClVCl valence angles are approximately equal, the VCl<sub>3</sub> fragment has been tilted relative to the V–C <sub>$\alpha$</sub>  bond axis in such a way that the nonbonded C <sub>$\beta$</sub> H<sub>3</sub>···Cl'' distance has increased (see Table 5 and Supporting Information). A similar distortion is found in the Ti analogue when the TiCC angle is reduced to 87°. The HOMO's of **7** and **8** both correspond to a nearly pure d<sub>xy</sub> orbital on the metal atom with a small admixture of antibonding interaction with Cl p orbitals. Introduction of the additional electron is thus expected to weaken the M–Cl bonds. Inspection of Figure 5 also suggests that Coulomb repulsion between the d<sub>xy</sub> electron density and the M–Cl''  $\sigma$ -bonding electrons would tend to increase the C <sub>$\alpha$</sub> MCl'' angle. Indeed, the C <sub>$\alpha$</sub> MCl'' angle of the *anagostic* equilibrium structure of EtVCl<sub>3</sub> is 107.9°, as compared with 105.6° in the Ti analogue. Accordingly we suggest that the presence of the additional electron lowers the energy required for distortion of the metal atom coordination geometry accompanying a reduction of the MCC angle.

(29) Endo et al. have optimized at the MP2 level a C<sub>s</sub> model of **7** with the ethyl group locked in the eclipsed conformation and obtained geometric parameters in reasonable agreement with ours; see ref 20a.

(30) The torsional mode in EtVCl<sub>3</sub> has a very low frequency, however, and it is impossible to exclude the possibility that calculations at a higher level would convert the staggered model to a transition state for methyl group rotation.

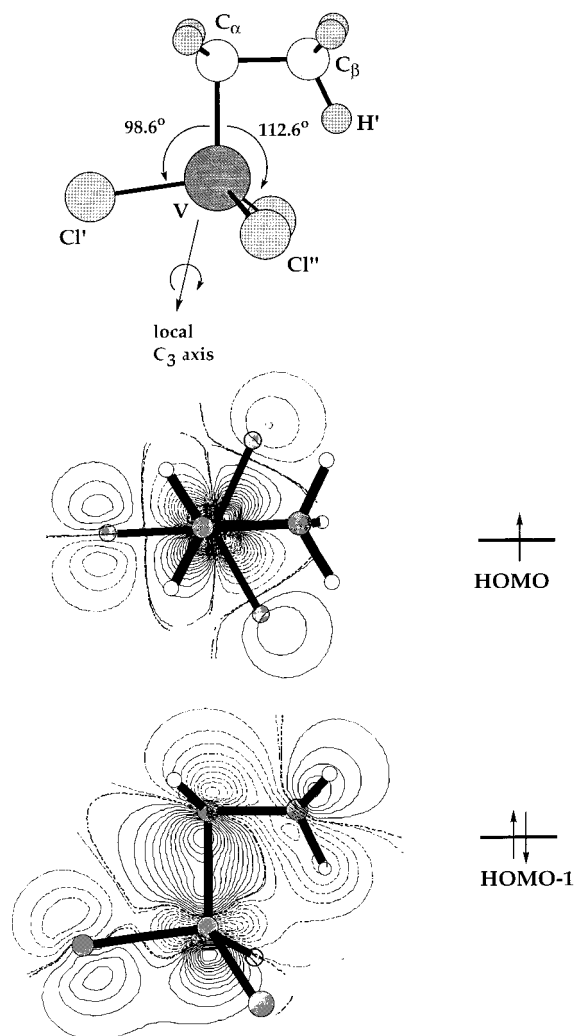


**Figure 5.** Top: coordination geometry of the eclipsed (agostic) conformer of EtVCl<sub>3</sub> (**7**). Bottom: contour maps of frontier MO's; the HOMO of EtVCl<sub>3</sub> contributes to a weakening of the V-Cl bonds and a widening of the C<sub>α</sub>VCl'' valence angles.

This hypothesis may also provide an explanation for the agostic nature of [EtVCl<sub>3</sub>]<sup>+</sup>. For four-coordinate complexes, therefore, it would seem that a flexible coordination geometry is more important for the adoption of an agostic structure than is a net positive charge on the metal atom.

### 3. Conclusions

We have drawn on DFT calculations, together with the structures and spectroscopic properties determined by experiment, to probe the nature and incidence of  $\beta$ -agostic interactions affecting ethyl groups coordinated to an early transition metal M. Our analysis has sought specifically to examine how such interactions vary with the atomic number, coordination number, valence electron (VE) count, and net charge on M.

$\beta$ -Agostic behavior appears in practice to require that the valence shell of M be unsaturated with VE  $\leq$  16. It is most prone to occur when M is three-coordinated, being seldom encountered in four- and six-coordinated systems (with only one example of each having been registered), and unknown in five-coordinated systems. Our DFT calculations on the three model three-coordinated complexes [EtTiCl<sub>2</sub>]<sup>+</sup>, EtScCl<sub>2</sub>, and EtTiCl<sub>2</sub> yield agostic structures with MCC angles of about 85° and eclipsed ethyl group conformations; the strength of the interaction varies in the order



The constant-probability-density contours imply that the HOMO in each of the d<sup>0</sup> species [EtTiCl<sub>2</sub>]<sup>+</sup> and EtScCl<sub>2</sub> is an M-C<sub>α</sub> bonding orbital which is delocalized over the entire ethyl group; it may be described as a combination of a nearly pure d<sub>z<sup>2</sup></sub> orbital on M with a C-C antibonding but C-H bonding orbital ( $\pi^*$ ) on the ethyl ligand. Canting of the ethyl group to establish an agostic structure leads to a covalent interaction between the C<sub>β</sub>H<sub>3</sub> fragment and the torus of the d<sub>z<sup>2</sup></sub> orbital on M. Even though the favored conformation of the ethyl group is such that one C<sub>β</sub>-H bond is pointing toward the metal atom, rotation of the C<sub>β</sub>H<sub>3</sub> group by 60° to generate the staggered conformer is not opposed by a significant barrier and does not necessarily result in a widening of the MCC valence angle. Assumption of a positive charge by the complex evidently strengthens the agostic interaction, Coulomb attraction between M and C<sub>β</sub> possibly augmenting the covalent attraction.

DFT calculations on four-coordinated complexes of the type [EtMCl<sub>3</sub>]<sup>n+</sup> (n = 0, M = Ti, V, Zr or Nb; n = 1, M = V) show that an agostic equilibrium structures are the rule. However, EtNbCl<sub>3</sub> is predicted to have a weakly agostic structure with  $\angle$ NbCC = 91.9° and an eclipsed ethyl group conformation, and EtVCl<sub>3</sub> to show incipient agostic behavior since a conformer with  $\angle$ VCC = 91.1° and an eclipsed ethyl group is calculated to lie only 0.76 kcal mol<sup>-1</sup> above the global minimum. The properties of these four-coordinated complexes may be rationalized if it is assumed that the reduction of the MCC angle is opposed by repulsion between the C<sub>β</sub>H<sub>3</sub> group and the two out-of-plane Cl atoms. Such repulsion may be alleviated either (i) by replacing a Fourth Period element like Ti or V by its Fifth Period congener Zr or Nb to create more space around the metal center or (ii) by replacing a d<sup>0</sup> by a d<sup>1</sup> metal center (e.g., Ti or Zr by V or Nb) to create a less rigid coordination geometry. Space and skeletal flexibility appear to be more important considerations here than does the assumption of a positive charge on M.

These same influences appear also to be decisive in transforming the agostic behavior of four-coordinated EtTiCl<sub>3</sub>, with VE = 8, into the  $\beta$ -agostic behavior clearly and uniquely authenticated for the six-coordinated complex EtTiCl<sub>3</sub>(dmpe), VE = 12. For DFT calculations suggest that coordination of the diphosphine *opens out* the coordination geometry of the metal atom and also renders it more pliable, thereby leading to a reduction of the forces opposing  $\beta$ -agostic interaction.<sup>31</sup> The structure [ $\angle$ TiCC = 84.57(9)°; eclipsed ethyl group]<sup>5</sup> and spectroscopic properties of the dmpe complex are well reproduced by the calculations which reveal, in addition, the existence of a second conformer with  $\angle$ TiCC = 93.1° and a staggered ethyl group only slightly less stable than the first, and which may be expected to participate in the solution chemistry of the complex.

In summary, therefore, the calculations reveal that agostic stabilization derives not from C-H  $\rightarrow$  M electron donation but from delocalization of the M-C bonding orbital, usually the HOMO in d<sup>0</sup> complexes. The bonding between the metal atom and the ethyl group is effectively provided by one electron pair

(31) On the basis of extended Hückel calculations, Eisenstein and co-workers have suggested that canting of the alkyl group is favored by the presence of a ligand in the trans position: Eisenstein, O.; Jean, Y. *J. Am. Chem. Soc.* **1985**, *107*, 1177-1186. The presence of a P atom trans to the ethyl group in **2** may well reduce the factors opposing the  $\beta$ -agostic interaction, but this is unlikely to be the dominant factor since DFT calculations at the BPW91 level indicate that the equilibrium geometry of a model of EtTiCl<sub>3</sub>(PH<sub>3</sub>) with a phosphine ligand trans to the ethyl group is anagostic.

and one orbital on the metal. Factors such as the Lewis acidity or VE count of the metal center are not decisive; instead, the form and rigidity of the metal–ligand framework appear to be crucial factors in permitting or inhibiting the development of the interaction. It remains to be seen how far the conclusions we have reached regarding the nature of  $\beta$ -agostic bonding are applicable to  $\alpha$ -,  $\gamma$ -, and other types of agostic interaction<sup>1</sup> and also to late transition-metal systems.

#### 4. Experimental Section

**Synthesis of EtTiCl<sub>3</sub> and EtTiCl<sub>3</sub>(dmpe).** Standard Schlenk and rigorous high-vacuum techniques were used throughout. EtTiCl<sub>3</sub> was prepared by the literature method exploiting the reaction between tetraethyllead and titanium tetrachloride.<sup>32</sup> In this method a molar excess of TiCl<sub>4</sub> is required to remove the alkylating agent and prevent the formation of di- or triethyltitanium derivatives. In practice, samples of EtTiCl<sub>3</sub> prepared via this route were invariably contaminated with substantial amounts (5–10%) of TiCl<sub>4</sub> impurity. This was removed by repeated fractional condensation in vacuo, the EtTiCl<sub>3</sub> being retained by a trap held at 228 K. The purity of the sample was checked carefully by reference to the <sup>1</sup>H NMR spectrum of a CD<sub>2</sub>Cl<sub>2</sub> solution<sup>32</sup> and to the IR spectrum of the vapor.<sup>6,33</sup> Deuterated samples of EtTiCl<sub>3</sub> were prepared in an analogous manner, the corresponding isotopomer of Et<sub>4</sub>Pb being synthesized by the reaction of Pb(OAc)<sub>4</sub> with a THF solution of the appropriate version of EtMgCl (itself prepared from CHD<sub>2</sub>CD<sub>2</sub>-Cl or CH<sub>2</sub>DCH<sub>2</sub>Cl).<sup>34</sup> The adducts CH<sub>3</sub>CH<sub>2</sub>TiCl<sub>3</sub>(dmpe), CHD<sub>2</sub>CD<sub>2</sub>-TiCl<sub>3</sub>(dmpe), and CH<sub>2</sub>DCH<sub>2</sub>TiCl<sub>3</sub>(dmpe) were prepared from the corresponding pure ethyltitanium trichloride by methods described previously.<sup>14</sup>

**Structure Determination and Spectroscopic Measurements.** Essential details of the structure determinations carried out on gaseous EtTiCl<sub>3</sub> (by electron diffraction at Oslo) and on a single crystal of EtTiCl<sub>3</sub>(dmpe) at 105 K (by X-ray diffraction at Munich) are to be found elsewhere.<sup>5</sup> NMR spectra of CD<sub>2</sub>Cl<sub>2</sub> solutions of EtTiCl<sub>3</sub> and EtTiCl<sub>3</sub>(dmpe) and their specifically deuterated isotopomers were recorded at Oxford with the aid of a Bruker AM-300 (300 MHz) or a Varian 500 (500 MHz) FT-NMR spectrometer. Infrared spectra were measured with a Mattson "Galaxy" FT-IR spectrometer, typically at a resolution of 2 cm<sup>-1</sup>.

**Quantum-Chemical Calculations.** Gaussian 94<sup>35</sup> DFT calculations were carried out using the BPW91 density functional with the gradient correction of Becke<sup>36</sup> for exchange and of Perdew-Wang<sup>37c</sup> for correlation. Basis set information is listed in the Supporting Information. Unless specified otherwise in the text we employed the basis set combination denoted "I"<sup>38–40</sup> for calculations on compounds EtTiH<sub>3</sub>, **1**, **2a**, **3–5**, **7**, and **9** and basis set combination "II"<sup>41,42</sup> for compounds **6** and **8**.

(32) Erskine, G. J.; Vanstone, N. B.; McCowan, J. D. *Inorg. Chim. Acta* **1983**, *75*, 159–162.

(33) McGrady, G. S.; Downs, A. J.; McKean, D. C.; Scherer, W. Unpublished results.

(34) Williams, K. C. *J. Org. Chem.* **1967**, *32*, 4062–4063.

(35) Frisch, M. J.; Trucks, G. W.; Schlegel, H. B.; Gill, P. M. W.; Johnson, B. G.; Robb, M. A.; Cheeseman, J. R.; Keith, T.; Petersson, G. A.; Montgomery, J. A.; Raghavachari, K.; Al-Laham, M. A.; Zakrzewski, V. G.; Ortiz, J. V.; Foresman, J. B.; Cioslowski, J.; Stefanov, B. B.; Nanayakkara, A.; Challacombe, M.; Peng, C. Y.; Ayala, P. Y.; Chen, W.; Wong, M. W.; Andres, J. L.; Replogle, E. S.; Gomperts, R.; Martin, R. L.; Fox, D. J.; Binkley, J. S.; Defrees, D. J.; Baker, J.; Stewart, J. P.; Head-Gordon, M.; Gonzales, C.; Pople, J. A. Gaussian 94, Revision C.2; Gaussian, Inc.: Pittsburgh, PA, 1995.

(36) (a) Becke, A. D. *Phys. Rev.* **1988**, *A38*, 3098–3100. (b) Becke, A. D. *ACS Symp. Ser.* **1989**, *394*, 165–179. (c) Becke, A. D. *Int. J. Quantum Chem.* **1989**, *Symposium No. 23*, 599–609.

(37) (a) Perdew, J. P. *Phys. Rev.* **1986**, *B33*, 8822–8824. (b) Perdew, J. P. *Phys. Rev.* **1986**, *B34*, 7406. (c) Perdew, J. P.; Wang, Y. *Phys. Rev.* **1992**, *B45*, 13244–13249.

(38) Wachters, A. J. H. *J. Chem. Phys.* **1970**, *52*, 1033–1036.

(39) McLean, A. D.; Chandler, G. S. *J. Chem. Phys.* **1980**, *72*, 5639–5648.

DFT calculations on **2** made use of the program system ADF.<sup>43</sup> The Vosko–Wilk–Nusair parametrization,<sup>44</sup> with the gradient corrections of Becke<sup>36</sup> for exchange and of Perdew<sup>37a,b</sup> for correlation, was used for the exchange-correlation energies (denoted as BP86 in the following). The gradient corrections were included self-consistently. The accuracy of the numerical integration was set to 10<sup>-4.0</sup> for each integral. This is assumed to give a numerical noise level of less than 0.5 kcal mol<sup>-1</sup> in the final energies.<sup>43e</sup> We employed a triple- $\zeta$  valence basis on Ti and double- $\zeta$  valence plus polarization on the other atoms. The atomic orbitals up to 2p were frozen on Ti, V, and Cl, while 1s was kept frozen on C. This basis set combination is designated "III".

The initial optimizations on all compounds were achieved without symmetry restriction and started from geometries without any symmetry. Invariably, however, the optimization of **1**, **3–6**, **8**, and **9** converged to C<sub>s</sub> symmetry. The final molecular geometry of each of these compounds was therefore optimized within the constraints of the C<sub>s</sub> point group. The DFT Cartesian force constants and Cartesian dipole moments for **1**, **2a**, and **3–9** were determined at the theoretical equilibrium geometries.

<sup>13</sup>C and <sup>1</sup>H chemical shifts were calculated at the BPW91/I level of theory for the BPW91/I- or BP86/III-optimized structures using the Gauge-Independent Atomic Orbital (GIAO) method in Gaussian 94. Chemical shifts are given with respect to TMS at the same computational level. Absolute shieldings of carbon and hydrogen in TMS at the BPW91/I level are 183.3 (C) and 31.96 (H).

**Acknowledgment.** We are grateful to the Deutsche Forschungsgemeinschaft for a postdoctoral fellowship (to W.S.), to Jesus College, Oxford for a research fellowship (to G.S.M.), to the EPSRC for assistance with the purchase of equipment, to the VISTA program of STATOIL and the Norwegian Academy of Science and Letters for financial support, and to the Research Council of Norway for a generous grant of computing time. We thank Prof. Malcolm Green, Prof. Donald McKean, and Dr. John Turner for helpful discussions and the referees for constructive comments and suggestions.

**Supporting Information Available:** Observed and calculated C–H(D) stretching frequencies for the ethyl groups of EtTiCl<sub>3</sub> (**1**), CHD<sub>2</sub>CD<sub>2</sub>TiCl<sub>3</sub> (**1-h<sub>1</sub>**), EtTiCl<sub>3</sub>(dmpe) (**2**), and CHD<sub>2</sub>CD<sub>2</sub>TiCl<sub>3</sub>(dmpe) (**2-h<sub>1</sub>**) and calculated scaled harmonic frequencies for **1**, **1-h<sub>1</sub>**, EtTiCl<sub>3</sub>(dhpe) (**2a**), and CHD<sub>2</sub>CD<sub>2</sub>TiCl<sub>3</sub>(dhpe) (**2a-h<sub>1</sub>**); GIAO chemical shifts at the DFT level for Me<sub>2</sub>TiCl<sub>2</sub>, MeTiCl<sub>3</sub>, EtTiCl<sub>3</sub> (**1**), and EtTiCl<sub>3</sub>(dmpe) (**2**); optimized geometries of EtTiCl<sub>3</sub> (**1**) and EtVCl<sub>3</sub> (**7**) at different computational levels; salient structural parameters for EtScCl<sub>2</sub> (**4**) and EtTiCl<sub>2</sub> (**5**); and Gaussian basis sets employed for calculations (6 pages). See any current masthead page for ordering and Web access instructions.

JA9737578

(40) Krishnan, R.; Binkley, J. S.; Seeger, R.; Pople, J. A. *J. Chem. Phys.* **1980**, *72*, 650–654.

(41) (a) Hay, P. J.; Wadt, W. R. *J. Chem. Phys.* **1985**, *82*, 270–283. (b) Wadt, W. R.; Hay, P. J. *J. Chem. Phys.* **1985**, *82*, 284–298. (c) Hay, P. J.; Wadt, W. R. *J. Chem. Phys.* **1985**, *82*, 299–310.

(42) Dunning, T. H., Jr.; Hay, P. J. In *Modern Theoretical Chemistry*; Schaefer, H. F., III, Ed.; Plenum: New York, 1976; pp 1–28.

(43) (a) Amsterdam Density Functional (ADF) Release 1.1.2, Department of Theoretical Chemistry, Vrije Universiteit, de Boelelaan 1083, 1081 HV Amsterdam, Netherlands. (b) Baerends, E. J.; Ellis, D. E.; Ros, P. *Chem. Phys.* **1973**, *2*, 41–51. (c) Baerends, E. J. Ph.D. Thesis, Vrije Universiteit Amsterdam, 1975. (d) Ravenek, W. In *Algorithms and Applications on Vector and Parallel Computers*; te Riele, H. J. J., Dekker, Th. J., van de Vorst, H. A., Eds.; Elsevier: Amsterdam, 1978. (e) te Velde, G.; Baerends, E. J. *J. Comput. Phys.* **1992**, *99*, 84–98.

(44) Vosko, S. H.; Wilk, L.; Nusair, M. *Can. J. Phys.* **1980**, *58*, 1200–1211.